

In presenting the dissertation as a partial fulfillment of the requirements for an advanced degree from the Georgia Institute of Technology, I agree that the Library of the Institution shall make it available for inspection and circulation in accordance with its regulations governing materials of this type. I agree that permission to copy from, or to publish from, this dissertation may be granted by the professor under whose direction it was written, or, in his absence, by the dean of the Graduate Division when such copying or publication is solely for scholarly purposes and does not involve potential financial gain. It is understood that any copying from, or publication of, this dissertation which involves potential financial gain will not be allowed without written permission.

EXPERIMENTAL DETERMINATION OF BOUNDARY-  
SHEAR STRESS OF OSCILLATORY FLOW IN  
A PIPE

A THESIS

Presented to  
The Faculty of the Graduate Division  
by  
James Otis Keniston

In Partial Fulfillment  
of the Requirements for the Degree  
Master of Science in Civil Engineering

Georgia Institute of Technology

December, 1963

EXPERIMENTAL DETERMINATION OF BOUNDARY-

SHEAR STRESS OF OSCILLATORY FLOW IN

A PIPE

Approved:

Chairman

Date Approved by Chairman September 21, 1965

## ACKNOWLEDGEMENTS

The writer is grateful to all those who made this thesis possible. Sincere appreciation is expressed to Dr. M. R. Carstens, the thesis advisor, for his able assistance throughout this study. Further appreciation is expressed to Mr. H. J. Bates, laboratory technician; Professor C. S. Martin, and fellow graduate students Mr. R. A. Coleman and Mr. A. K. Rajpal.

Dr. Carstens, Professor C. E. Kindsvater, and Professor Martin served as members of the thesis reading committee.

The writer also wishes to thank the National Science Foundation for the material support which made this thesis possible.

## TABLE OF CONTENTS

	page
ACKNOWLEDGMENTS.....	ii
LIST OF TABLES.....	iv
LIST OF FIGURES.....	v
LIST OF SYMBOLS.....	vi
SUMMARY.....	viii
CHAPTER	
I. INTRODUCTION.....	1
II. THE EQUATION OF MOTION.....	4
III. INSTRUMENTATION AND EQUIPMENT.....	8
The Driving End	
The Reservoir End	
Design of the Test Section	
The Test Section	
Instrumentation	
IV. EXPERIMENTAL PROCEDURE.....	20
V. ANALYSIS OF DATA.....	25
The Pressure Calibration Curve	
Analysis of the Pressure Record	
VI. ANALYSIS AND DISCUSSION OF RESULTS.....	32
Discussion of Results	
Discussion of the Fluctuations in the Pressure Record	
VII. CONCLUSIONS.....	41
BIBLIOGRAPHY.....	42

## LIST OF TABLES

Table	Page
1. Calibration Data.....	33

## LIST OF FIGURES

Figure	Page
1. Free-Body Diagram of Fluid Element .....	5
2. Photograph of Assembled Apparatus .....	9
3. Photograph of the Driving End .....	10
4. Design Curve Obtained from the Theoretical Laminar Solution ...	15
5. Detail Drawing of Piezometers .....	17
6. Schematic Drawing of Assembled Apparatus .....	19
7. Calibration Curve .....	22
8. Sample of Pressure Record .....	24
9. Plot of Shear Versus $\omega t$ for One Complete Cycle in Run No. 2 ( $0 \leq \omega t \leq 2\pi$ ) .....	27
10. Plot of Shear Versus $\omega t$ (Run No. 1) .....	29
11. Plot of Shear Versus $\omega t$ (Run No. 2) .....	30
12. Plot of Shear Versus $\omega t$ (Run No. 3) .....	31
13. Free-Body Diagram of Annular Fluid Element Adjacent to Pipe Wall .....	34
14. A Plot of Shear Stress Gradient Versus $\omega t$ for Decelerated Flow .....	36
15. Shear and Velocity Profiles for Experiment 1 .....	37
16. The Theoretical Velocity Profiles of Laminar Flow for Various Values of $\omega t$ .....	39

## LIST OF SYMBOLS

A	cross-sectional area of the pipe
$a_0$	half amplitude of fluid in the pipe
$C_L$	cycle length on pressure record in cm
C	constant in the theoretical laminar solution
D	internal diameter of the pipe
E	constant in the theoretical laminar solution
f	Darcy-Weisbach resistance coefficient
L	length of fluid element
P	half amplitude of pressure gradient in laminar flow
$p^*$	piezometric pressure
$r_0$	radius of pipe
r	radial distance from pipe centerline
R	$VD/\nu$ = Reynolds number
t	time
T	period of oscillation
v	axial velocity of fluid at a point
V	mean velocity of fluid in pipe at any time
V	volume of fluid element
$X_L$	distance in cm from origin to point under consideration on pressure record
y	ordinate on pressure record
z	distance along the axial direction in the pipe
$\ddot{z}$	axial acceleration in the pipe
$\alpha_i$	root of $J_0(X) = 0$ $J_0(\alpha_i) = 0$



- $\beta$   $r/r_o$
- $\nu$  kinematic viscosity of the fluid
- $\phi$  phase angle between pressure and acceleration
- $\rho$  mass density of the fluid
- $\tau$  shear stress
- $\omega$  angular velocity
- $X$  stability parameter
- $o$  subscript denoting position at the pipe wall
- $s$  subscript denoting steady flow
- $u$  subscript denoting unsteady flow
- $1,2$  subscript denoting location of section

## SUMMARY

An experimental investigation was made to determine the boundary shear stress for unsteady turbulent flow in a pipe. In the past the main difficulty encountered in any unsteady shear stress investigation was the evaluation of the inertia of the fluid element. In this study, the problem was approached by oscillating the fluid simple-harmonically in the pipe. The reason for selecting this mode of oscillation was the fact that the mean acceleration of the fluid in the pipe would become an independent programmed variable. The pressure gradient in the pipe was measured by means of transducers attached to piezometers on the pipe. Since both the inertia and pressure gradient are measurable, a momentum analysis can be applied to the fluid element in the pipe. Thus, the boundary shear stress is the only unknown in the resulting equation.

The main difficulty encountered in the experiments was the appearance of intense fluctuations in the pressure record. These fluctuations appeared shortly before the fluid changed direction in the pipe, remained until the fluid had reached maximum velocity in the test section, and disappeared as the fluid began decelerating. Due to these disturbances, results could only be obtained for decelerated flows.

Experiments were performed for three different periods of oscillation. The following conclusions were reached:

- (a) The boundary shear stress for turbulent, decelerated flow is essentially equal to the equivalent steady flow values.

(b) The shear force for turbulent, oscillatory flows reverses direction approximately ten degrees before the mean velocity of the fluid.

## CHAPTER I

### INTRODUCTION

#### Statement of the Problem

The purpose of this study was to compare the boundary-shear stress of a particular unsteady turbulent flow with the corresponding well-known values of steady flow. The study of boundary-shear stress for unsteady turbulent flow in a pipe is tractable only by the experimental method. In these experiments water was oscillated with simple harmonic motion in a straight smooth pipe. Utilizing the equation of motion, the boundary-shear stress was calculated, incorporating experimentally determined values of the pressure and inertia forces.

#### Review of the Literature

Carstens and Roller (1) studied accelerated flow in a smooth, straight, circular pipe. Their apparatus consisted of 1) a large reservoir in which the piezometric head was maintained constant, 2) a test section which was a section of smooth extruded brass pipe, 3) a group of piezometers spaced 95 diameters apart along the pipe, and 4) a quick-opening valve at the extreme end of the pipe. The piezometric head was sensed at the piezometers by means of electronic pressure transducers. The output from these transducers was amplified electronically and was recorded on a Sanborn two-channel oscillograph. The velocity of the effluent jet was determined by taking motion pictures of the effluent jet and using the free-fall equations. The linear-momentum equation was then

solved for values of the boundary shear stress using the values of pressure gradient and inertia obtained from experimental results. The results of this study seem to indicate that the unsteady-slow shear is slightly greater than the equivalent steady-flow shear when the fluid is accelerating. These results must be considered to be approximate because of the inaccuracy of the graphical method which had to be used to obtain the inertial term in the equation of motion.

Daily et al. (2) used a non-return, unsteady flow water tunnel to conduct their experiments. Their apparatus consisted of two cylindrical tanks connected by a test section of 1 inch diameter brass pipe which was 99 diameters in length. The driving force behind the accelerated or decelerated flow in the test section was obtained by admitting or withdrawing compressed air from one of the tanks. In order to obtain the desired acceleration or deceleration in the test section, the compressed air had to be admitted or released according to a definite time schedule. Discharge measurements were obtained by means of a streamlined nozzle placed at the inlet to the test section.

The flow meter readings were obtained with dynamic pressure measuring equipment. The pressure gradient along the test section was obtained by means of two transducers attached to piezometers on the test section. Thus the necessary data for evaluating unsteady-flow shear (namely pressure gradient and inertia) were obtained. The conclusions reached were: a) with acceleration the resistance is slightly, but not appreciably, greater than the equivalent steady state; b) with deceleration the resistance is appreciably less than for the equivalent steady state; and c) with either acceleration or deceleration it appears that

the internal flow structure is not markedly different from that for steady state.

## CHAPTER II

## THE EQUATION OF MOTION

Gross characteristics of unsteady flow in conduits can be readily studied experimentally provided that the test section is a uniform flow zone. This fact is clearly demonstrated by the equation of motion for an incompressible fluid in a circular pipe. The fluid free-body extends axially from cross section 1 to cross section 2 and radially to the pipe wall as shown in Figure 1.

The linear momentum equation for this fluid element is:

$$(p_1^* - p_2^*) \frac{\pi}{4} D^2 - \tau_0 \pi D L = \rho \frac{\partial}{\partial t} \int_V v dV \quad (1)$$

in which

- $p_1^*$  = piezometric pressure at section 1,
- $p_2^*$  = piezometric pressure at section 2,
- $D$  = internal diameter of the pipe,
- $\tau_0$  = boundary shear stress,
- $L$  = axial length between piezometer 1 and 2,
- $t$  = time,
- $\rho$  = mass density of fluid,
- $v$  = axial velocity of the fluid at a point, and
- $V$  = volume of the fluid element.

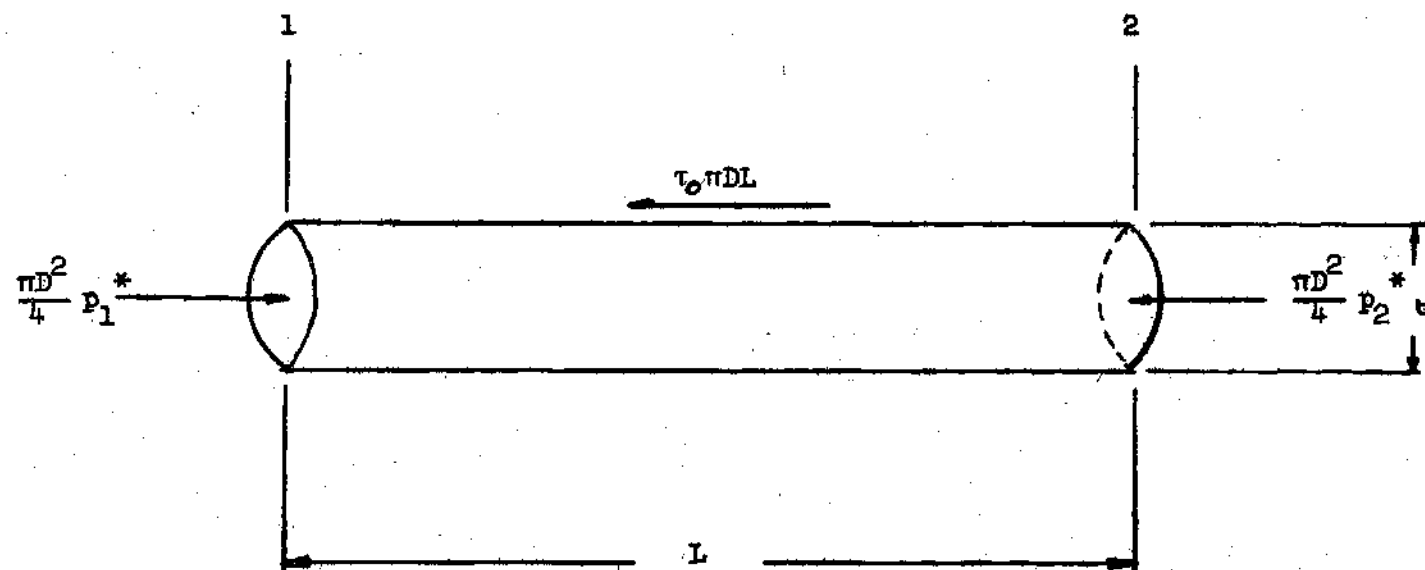


Figure 1. Free-Body Diagram of Fluid Element



The terms on the left hand side of equation (1) are the external forces. The first term is the combined pressure and weight force along the pipe axis. The second term is the boundary shear force.

The right hand side of equation (1) is the time-rate of change of linear momentum of the system of particles comprising the fluid element. Since the fluid element is in a uniform flow zone, the linear momentum flux out of the element equals the flux into the element. Consequently the only term appearing is that of the time rate of change of linear momentum within the fluid element. Since the velocity,  $v$ , is a function of radial position only, the following simplifications are possible:

$$\rho \frac{\partial}{\partial t} \int_V v dV = \rho L \frac{\partial}{\partial t} \int_A v dA = \rho L \frac{dQ}{dt} = \rho LA \frac{dv}{dt}$$

in which

$A$  = cross-sectional area of pipe,

$dA$  = differential cross-sectional area,

$Q = Q(t)$  = discharge or volume rate of flow, and

$V = Q/A = V(t)$  = mean velocity

The simplified equation of motion for unsteady flow in a circular pipe is

$$\frac{p_1^* - p_2^*}{L} - \frac{4\tau_0}{D} = \rho \frac{dv}{dt} \quad (2)$$

Equation (2) is valid for either laminar or turbulent flow. Solution is possible for any laminar flow for which the pressure gradient can be formulated as a function of time as demonstrated by Sneddon (3). By virtue of analytical solutions, boundary shear stress as a function of time can be determined for unsteady laminar flow in a pipe. In contrast, the boundary shear stress must be determined experimentally for all turbulent flows.

In any event, the boundary shear stress may be determined by means of equation (2) provided that the pressure gradient term,  $(p_1^* - p_2^*)/L$ , and the inertial term, can be determined. The pressure gradient as a function of time can be determined readily by means of commercially available instruments, whereas the change in mean velocity with respect to time is difficult to determine experimentally. As a result, a logical option is to construct the equipment such that  $dV/dt$  is an independent, programmed variable. Therefore, the apparatus used in these experiments was designed in such a way that the mean velocity,  $V$ , and  $dV/dt$  were made to vary in a known fashion; namely, simple harmonically.

### CHAPTER III

#### INSTRUMENTATION AND EQUIPMENT

The apparatus consists of three main groups which are: the driving end, the test section, and the reservoir end. Figure 2 is a picture of the assembled apparatus. Each group is discussed separately.

##### The Driving End

The driving end contains the mechanism which imposes simple harmonic motion on the fluid in the test section. Figure 3 is a picture of the driving end of the apparatus. The fluid is driven by a piston which has a stroke of 15.02 cm. This piston rides in a cylinder with an inside diameter of 3.062 in. The piston driving rod is attached to a scotch-yoke mechanism which is in turn driven by the drive motor. The angular speed of the drive shaft can be adjusted from 3.75 to 42 revolutions per minute. Attached to the bottom of the cylinder is a standard 3-in tee which is faced to receive a standard 3-in flange. The test section is attached to this tee.

##### The Reservoir End

The purpose of the reservoir end is to supply a positive pressure on the water in the test section at all times and to supply a place into which the water in the test section can flow. This end is housed in a stand which contains the following items; a standard 3-in tee to which the test section may be attached, a vertical cylinder with an inside

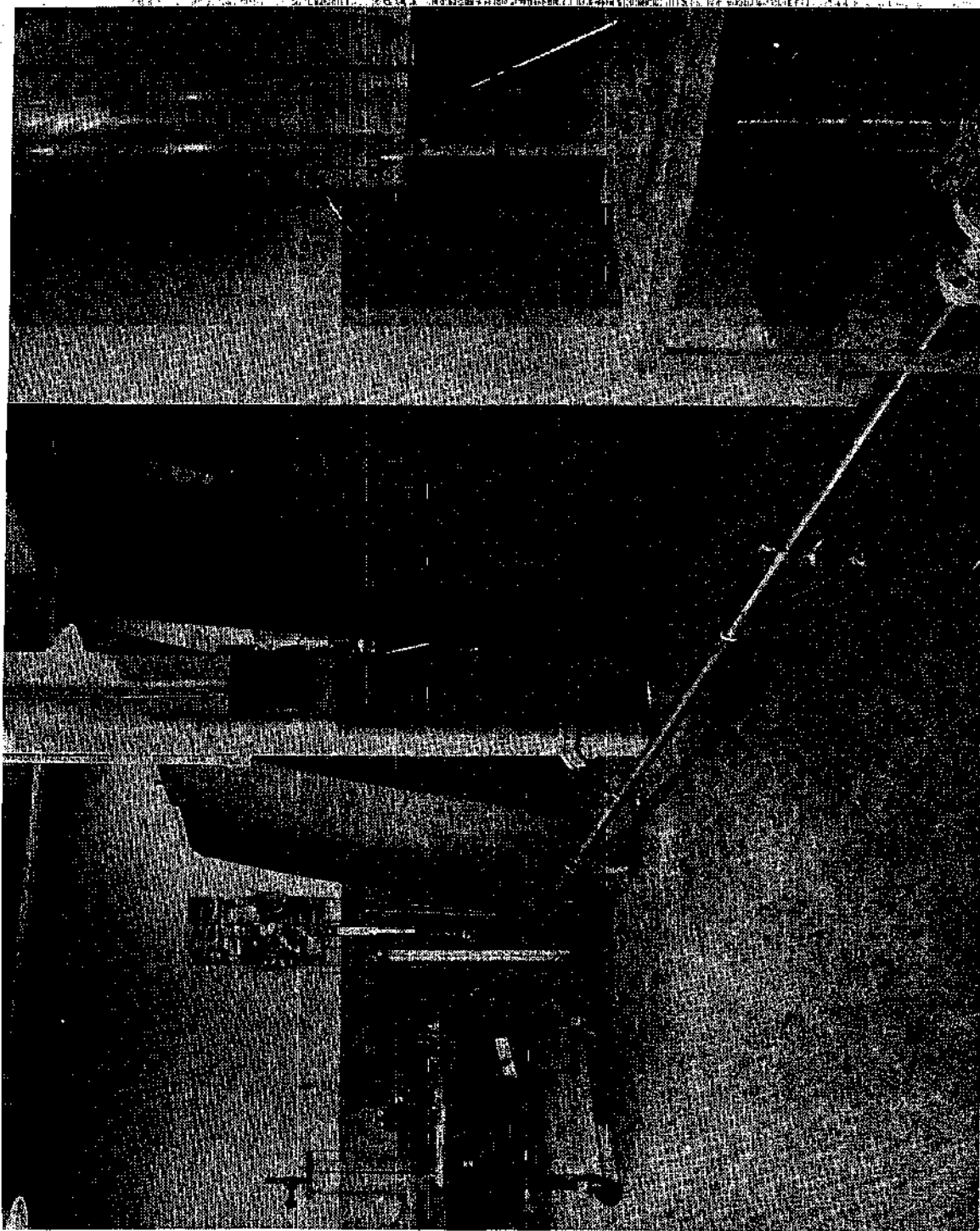


Figure 2. Photograph of Assembled Apparatus

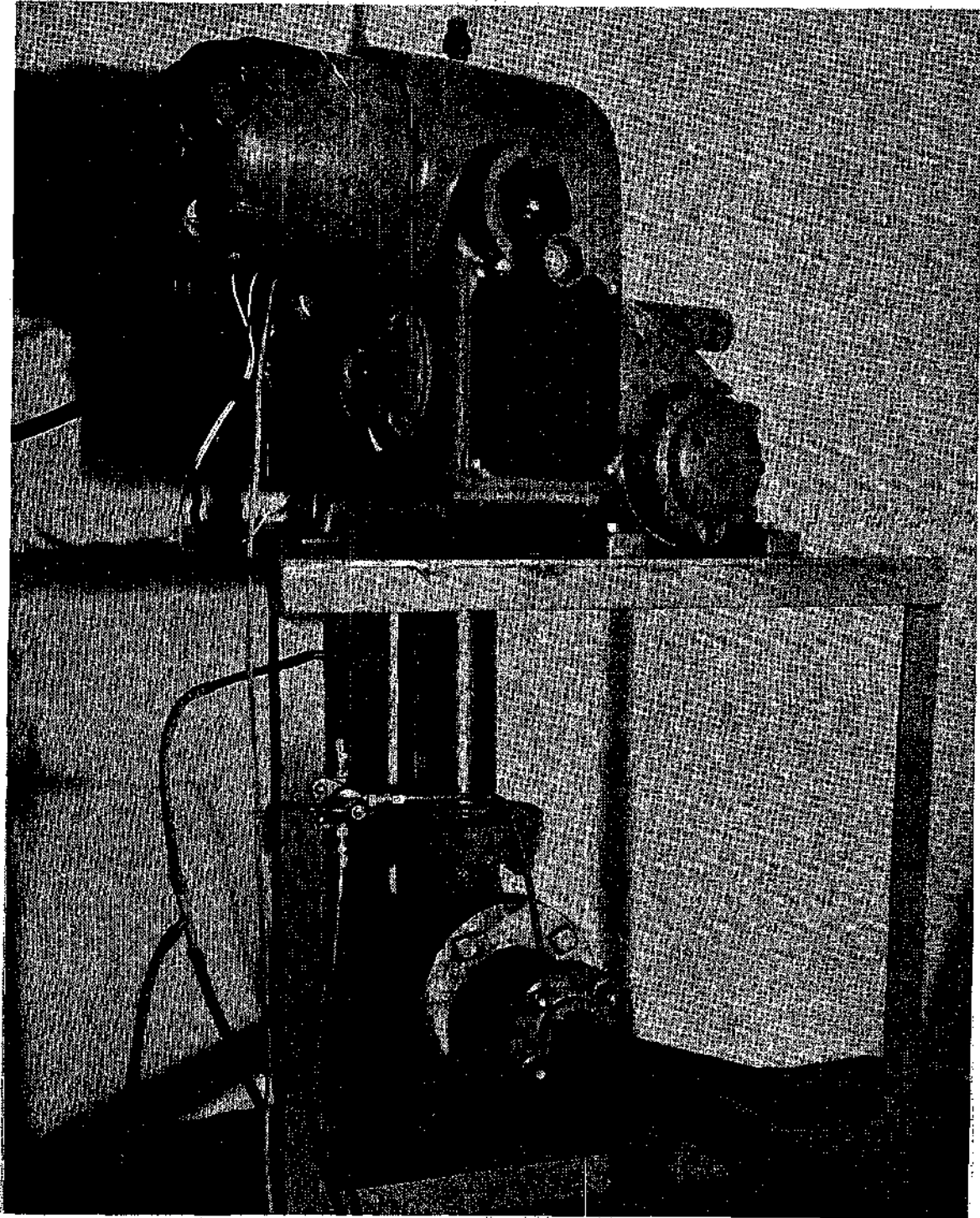


Figure 3. Photograph of Driving End

diameter of 3.062 in and a ten-foot length of clear plastic pipe which is attached directly in line with and above the cylinder.

#### Design of the Test Section

For this study two criteria must be satisfied. First, since this is a study of unsteady turbulent flow, the flow must be turbulent. Second, the maximum boundary shear stress must be a significant percentage of the maximum pressure gradient inasmuch as the boundary shear is computed by taking the difference between the pressure gradient term and the inertia term, equation (2).

To satisfy the first criterion, or that of having turbulent flow in the test section, a paper by C. S. Martin (4) was referred to. Martin applied Rouse's parameter (5) to the solution of the Navier-Stokes equations for two-dimensional, oscillatory laminar flow over a flat plate. The resulting stability parameter took the form,

$$X = 1.53a_o \sqrt{\frac{\omega}{2\nu}}$$

in which

$X$  = the stability parameter,

$a_o$  = half amplitude of travel of the fluid element in the test section,

$\omega$  = angular velocity, and

$\nu$  = kinematic viscosity of the fluid.

Martin stated that, when the value of  $X$  exceeded 400, the flow would likely be turbulent. It was determined that  $X$  would be greater than 400

at all available angular speeds of the drive unit if a pipe with an internal diameter less than or equal to 0.626 in was used.

The second criterion, or that of making the shear a significant part of the pressure, was approached by solving the Navier-Stokes equation for oscillatory laminar flow in a pipe. This seemed to be a safe design criterion due to the fact that the boundary-shear stress in laminar flow is always less than it would be in corresponding turbulent flow. In other words if the ratio of shear to pressure was found to be of sufficient magnitude from the laminar solution, this ratio would certainly be greater for corresponding turbulent flow.

The Navier-Stokes equation for two-dimensional flow in cylindrical co-ordinates has been solved using Fourier transform methods. The derivation and solution can be found in Sneddon (3). In this solution the pressure gradient can be any function of time. In this study the following form for the pressure gradient was chosen

$$\frac{\partial p^*}{\partial z} = P \sin (\omega t - \phi)$$

in which

$z$  = distance in axial direction,

$P$  = maximum pressure gradient, and

$\phi$  = phase angle between pressure and mean acceleration.

Neglecting transients, the solution is

$$v = \frac{2P}{\rho} \sum_{i=1}^{\infty} \frac{J_0(\alpha_i \beta)}{\alpha_i J_1(\alpha_i)} \left[ \frac{K \alpha_i^2 \sin(\omega t - \phi) + \omega \cos(\omega t - \phi)}{(K \alpha_i^2)^2 + \omega^2} \right] \quad (3)$$

in which

$r_o$  = radius of the pipe,

$K = \nu/r_o^2$

$\beta = r/r_o$ , and the

$\alpha_i$ 's are roots of the Bessel function  $J_0(X) = 0$   
solving for the mean velocity,  $V$ ,

$$V = \frac{1}{A} \int_A v dA = \frac{1}{\pi r_o^2} \int_0^{r_o} v(2\pi r) dr = 2 \int_0^1 v \beta d\beta \quad (4)$$

Substituting equation (3) into equation (4),

$$V = \frac{4PT}{\rho} \left[ C \sin(\omega t - \phi) - E \cos(\omega t - \phi) \right] \quad (5)$$

and

$$\tan \phi = C/E$$

in which

$$C = \sum_{i=1}^{\infty} \frac{\nu T / r_o^2}{\alpha_i^2 (\nu T / r_o^2)^2 \alpha_i^4 + (2\pi)^2}$$



$$E = \sum_{i=1}^{\infty} \frac{vT/r_o^2}{\alpha_i^2 \left[ (vT/r_o^2)^2 \alpha_i^4 + (2\pi)^2 \right]}$$

and

$T$  = period of oscillation.

Equation (5) can be differentiated to obtain the acceleration. Since the pressure gradient and acceleration are then known, equation (2) can be solved for the boundary shear stress. The equation thus obtained is a function of  $C$  and  $E$  only. Since  $C$  and  $E$  are both functions of  $vT/r_o^2$ , the ratio of maximum shear to maximum pressure for the theoretical solution can be determined as a function of  $vT/r_o^2$  also.

$$\frac{|4\tau_o/D|_{\max}}{|(p_1^* - p_2^*)/L|_{\max}} = \sqrt{1 + 8\pi^2(C^2 + E^2)} - 16\pi E \quad (6)$$

This ratio is plotted for values of  $vT/r_o^2$  ranging from 0.001 to 0.141 in Figure 4.

It was decided that the ratio of maximum shear to maximum pressure must be greater than 0.20. Referring to Figure 4, this condition can be fulfilled if  $\frac{vT}{r_o^2}$  is greater than or equal to 0.067. With a test section diameter of 0.626 in. and with water, the criterion for the magnitude of shear can be fulfilled if the minimum period,  $T$ , is 4.6 sec.

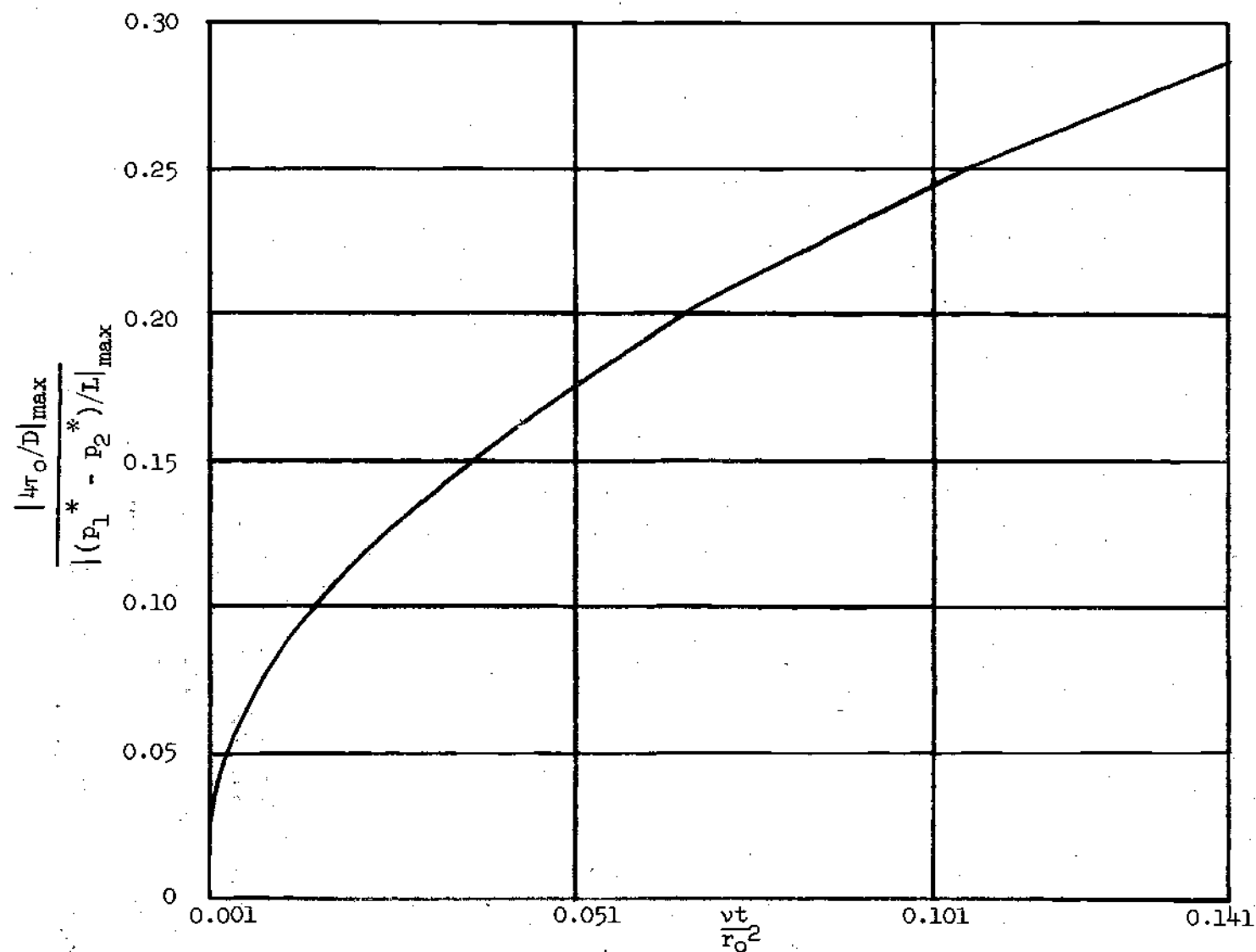


Figure 4. Design Curve Obtained from the Theoretical Laminar Solution

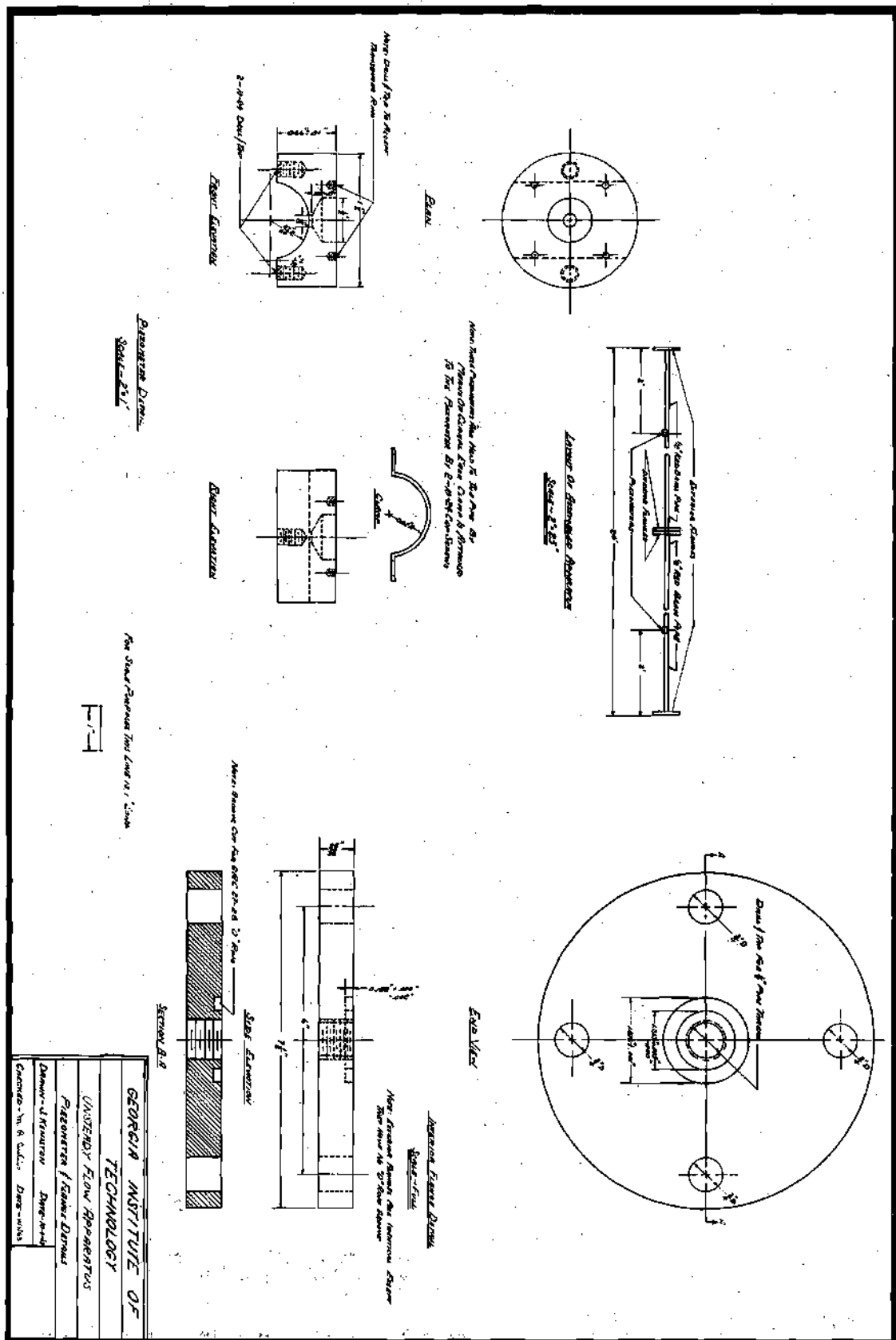
### The Test Section

In these experiments the test section consisted of two 12-ft lengths of seamless red-brass pipe with an inside diameter of 0.626 in. The central junction of the two pipes is made with two standard 3-in. blind flanges which are drilled and tapped to accept the pipe. The pipes are threaded into these flanges and the flanges are bolted together. The extreme ends of the assembled test sections are threaded into similarly prepared 3-in. flanges and these flanges are, in turn, joined to the flanged tees of the driving and reservoir ends, respectively. Figure 5 is a detailed drawing of the test section.

### Instrumentation

A mercury dip switch is used to give an indication on the pressure record when the piston is in midposition. The switch consists of a stainless-steel needle and a tube filled with mercury. The needle is attached to the piston rod such that it makes contact with the mercury surface when the piston is in midposition. The switch is wired to the remote marker on the Sanborn recorder. The pulse-marking channel in the recorder is activated when the needle is in contact with the mercury.

In order to obtain the piezometric pressure gradient along the test section, two piezometers are attached to the section at a spacing of 20.00 feet. Figure 5 is a drawing of these piezometers and their placement. Attached to each piezometer is a Consolidated Electrodynamic Pressure Transducer, type 4-312, with a range of  $\pm 7.5$  psi. The output from the two transducers is connected in series opposition to give the



algebraic difference between the two signals. The resulting signal is fed into a Sanborn direct-writing oscillograph. The deflection of the trace obtained is proportional to the pressure difference.

The filling and pressure-transducer calibrating equipment is shown in Figure 6. The water supply reservoir (1) is placed adjacent to the driving end and is used to fill or empty the apparatus. The manometry arrangements (2) are used to measure pressure differences when the transducers are being calibrated. In order to calibrate the transducers a metal plate (3) is placed between the central flanges (4). In order to fill or drain the equipment or to vary the pressure on the driving end of the test section during calibration the pump (5) can apply pressure or vacuum to the water in the water supply reservoir and this pressure can in turn be transmitted to the test section by opening valve (6). Valve (7) is opened while the equipment is being filled or if the head in the stand pipe end is varied during calibration.

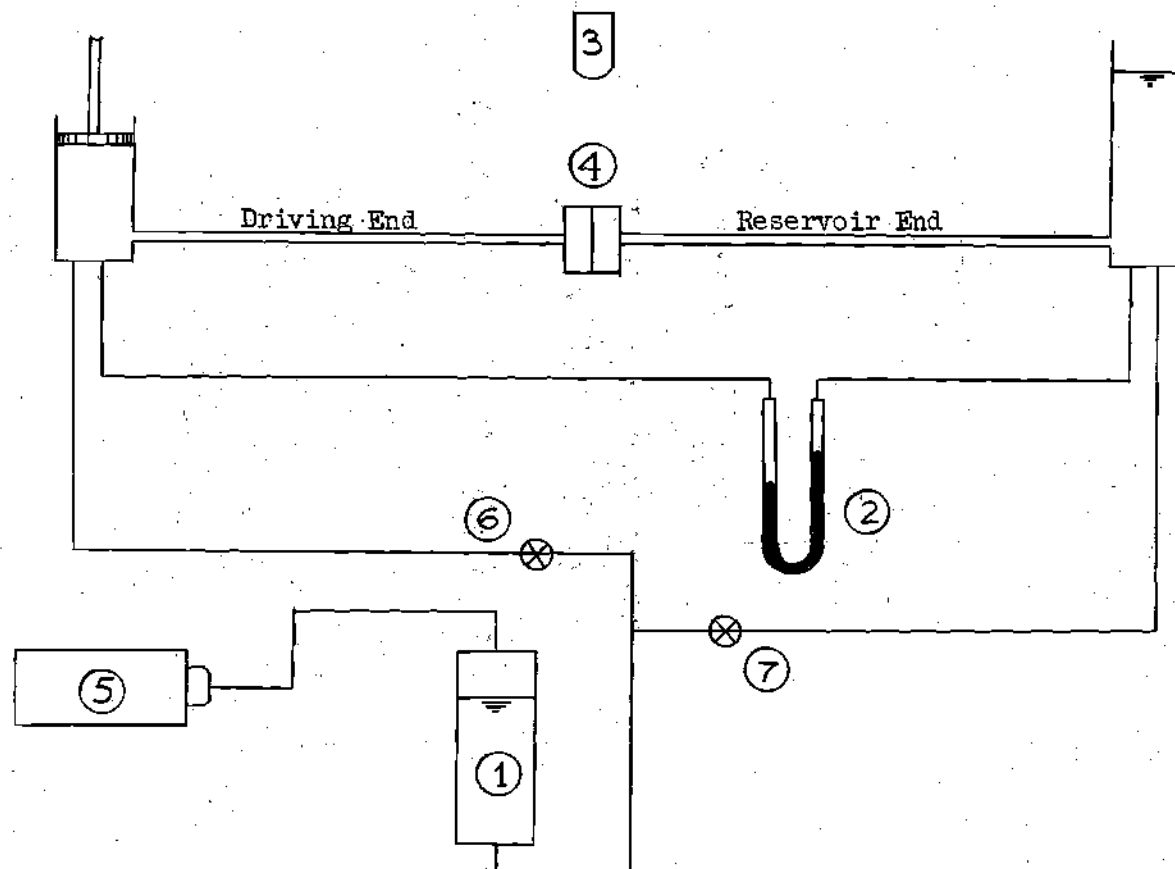


Figure 6. Schematic Diagram of Calibration Apparatus

## CHAPTER IV

## EXPERIMENTAL PROCEDURE

The pressure transducers were calibrated immediately prior to making a run in the following manner. As shown in Figure 6, the metal plate (3) was inserted between the central flanges (4). The pressure in the reservoir end was held constant by closing valve (7). The pressure in the driving end was varied by opening valve (6) and by varying the pressure or vacuum supplied to the system by the pump (5). For each established pump pressure in the driving end the elevation of the mercury surface in each leg of the mercury manometer was read to the nearest 0.005 cm by means of a cathetometer. The scribe on the oscillograph deflected for each differential value of pressure applied to the transducers. Thus a deflection on the oscillograph record corresponds to a given pressure difference. When the pressure in the driving end had been forced to assume four or five values both above and below the pressure in the standpipe end, the calibration was complete.

A run was executed as follows: The sheet steel was removed from between the central flanges. The bolts holding the junction together were tightened. The apparatus was filled until the water level in the standpipe was approximately five feet above the piston. Valves (6) and (7) were closed. The water temperature was recorded. The drive motor was started and the angular speed was increased until the desired deflection of the oscillograph scribe was attained. The leads from the mercury dip

switch were connected to the "remote marker" outlet on the recorder. The paper-feed motor in the recorder was run at its highest speed. When a pressure record had been obtained for a sufficient number of cycles (usually five or six), the drive motor was set at another speed and the process was repeated. When pressure records for the desired number of runs had been obtained, the drive motor was shut off and the mercury dip switch was disconnected. The automatic timer in the recorder was turned on with the paper-feed motor running in order to obtain the period of the oscillation.

The transducers were then recalibrated in the same manner as before and the final water temperature was recorded. Figure 7 is a plot of manometer deflection versus chart deflection,  $y$ . Using least-squares analysis, the equation for the best-fit straight line is obtained. The equation of the line is an equation of manometer deflection as a function of chart deflection. Using the manometer equation, the equation for pressure difference over a given length (in this case 20.00 ft.) as a function of  $y$  can be derived. Thus for any value of  $y$  on the pressure record the  $\frac{P_1^* - P_2^*}{L}$  term in the equation of motion can be evaluated. In the calibration runs conducted for these experiments the equation of the calibration curve was:

$$\frac{P_1^* - P_2^*}{L} = 11.04y - 25.37 \quad (7)$$



Equation for line is manometer deflection =  $19.584 - 8.608$  (chart deflection) or solving for  $\frac{p_1^* - p_2^*}{L}$ ,  $\frac{p_1^* - p_2^*}{L} = 11.037$  (chart deflection) - 25.342

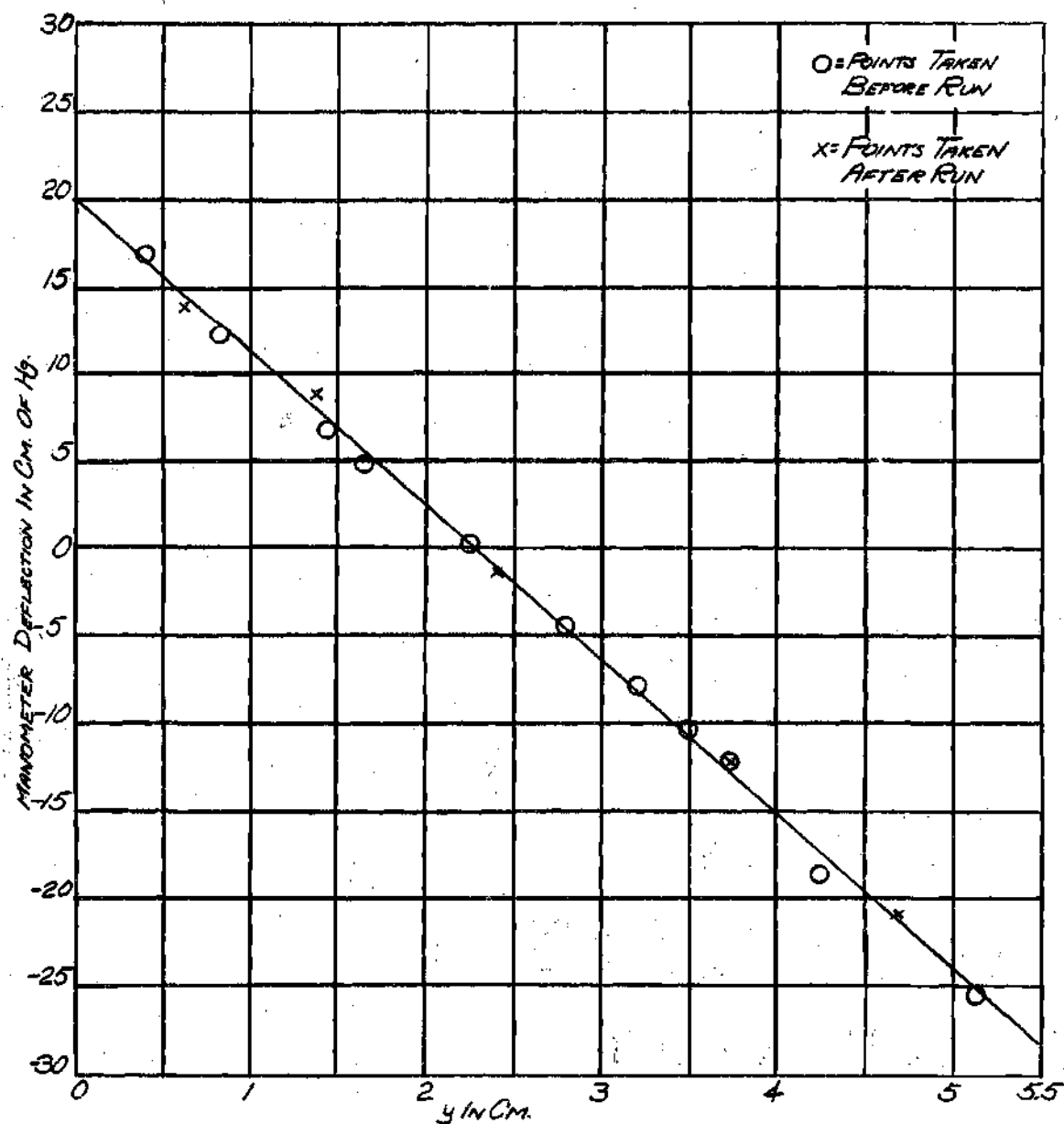


Figure 7. Calibration Curve

### Analysis of the Pressure Record

A typical sample of the pressure record obtained during one of the experiments is shown in Figure 8. The quantities in Figure 8 are defined as follows: The distance  $C_L$  is the distance in cm from the origin (the point where the stainless steel needle first makes contact with the mercury surface in the mercury dip switch) to the finish point or point where this occurs again. This distance is called the cycle length. Since the paper feed rate is known in cm of paper travel in one second, the time required for one cycle is readily obtainable. The distance of paper travel from the origin to the point in the cycle under consideration is designated as the distance  $X_L$ . The value,  $y$ , is the distance in cm from the bottom grid line on the record to the trace on the record corresponding to the pressure difference. Thus for every value of  $X_L$  within a given cycle there is a corresponding value of  $y$ .

When a cycle is analyzed, the following quantities are recorded;

a) the cycle length,  $C_L$ , and b)  $y$  and  $X_L$  for each mm of paper travel within the cycle.

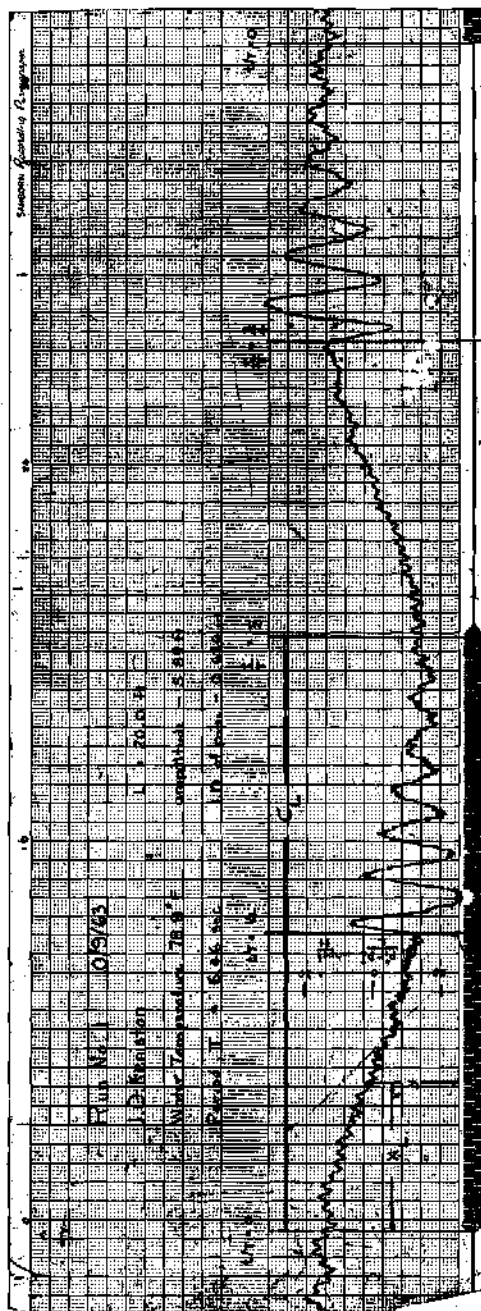


Figure 8. Sample of Pressure Record

## CHAPTER V

## ANALYSIS AND DISCUSSION OF RESULTS

Once the data have been taken from the pressure record, the results are obtained in the following manner. The equation of motion, equation (2), when rearranged and solved for  $4\tau_o/D$  takes the form;

$$\frac{4\tau_o}{D} = \frac{p_1^* - p_2^*}{L} - \rho \frac{dv}{dt}$$

The simple-harmonic motion relationships for the fluid element are;

$$z = a_o \sin(\omega t)$$

$$\dot{z} = V = a_o \omega \cos(\omega t)$$

$$\ddot{z} = -a_o \omega^2 \sin(\omega t)$$

in which

$z$  = axial displacement of fluid element from midposition,

$V$  = mean velocity of fluid in the test section,

$\frac{dv}{dt}$  = mean acceleration of fluid in test section,

$\omega t = 2\pi X_L / C_L$  (for analysis of pressure record),

$X_L$  = distance in cm from the origin of a cycle to the point in the cycle under consideration, and

$C_L$  = total length of cycle in cm.

The inertia term,  $\rho dv/dt$ , in the equation of motion becomes

$$\rho \frac{dv}{dt} = -\rho a_o \omega^2 \sin(2\pi X_L / C_L)$$

Equation (7) is used to evaluate the pressure gradient term

$$\frac{P_1^* - P_2^*}{L}$$

Since  $X_L$  and  $y$  are known for every millimeter of paper travel within a cycle, the instantaneous shear can readily be determined using the equation of motion in the following revised form:

$$\frac{4\tau_o}{D} = (11.04y - 25.3) + p a_o \omega^2 \sin(2\pi X_L / C_L)$$

Values of  $4\tau_o/D$  were evaluated for every data point of the three experiments. A plot of  $4\tau_o/D$  versus  $\omega t$  for Run number 2 is shown in Figure 9. A smooth curve can be drawn through the points in the ranges of  $\omega t$  from  $0^\circ$  to  $90^\circ$  and from  $180^\circ$  to  $270^\circ$ . However no curve will fit the values of shear in the ranges of  $\omega t$  from  $90^\circ$  to  $180^\circ$  and from  $270^\circ$  to  $360^\circ$ . Hence the data obtained are good only for decelerated flows. The results for decelerated flow are plotted to an exaggerated scale in Figures 10, 11, and 12.

In order to compare these results with those of steady flow having the same instantaneous mean velocity the Darcy-Weisbach equation was expressed in the following manner,

$$\tau_{ss} = \frac{f}{4} \frac{\rho V^2}{2}$$

in which  $\tau_{ss}$  = steady-flow shear stress, and  $f$  = resistance coefficient.

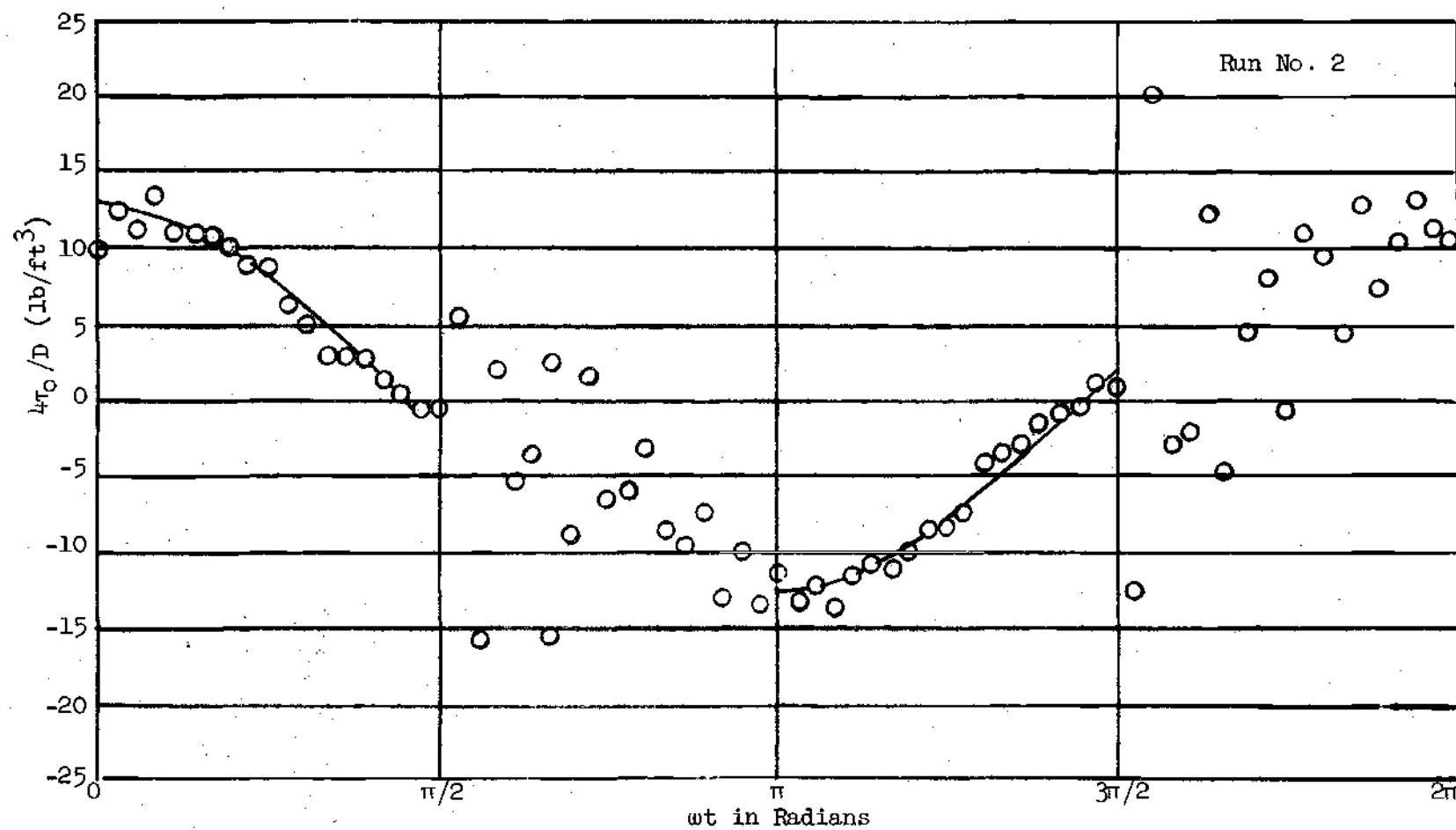


Figure 9. Plot of Shear Versus  $\omega t$  for One Complete Cycle in Run No. 2 ( $0 \leq \omega t \leq 2\pi$ )

Since the Reynolds number is never greater than 100,000, the Blasius equation is the best approximation of the resistance coefficient,

$$f = \frac{0.316}{R^{1/4}}$$

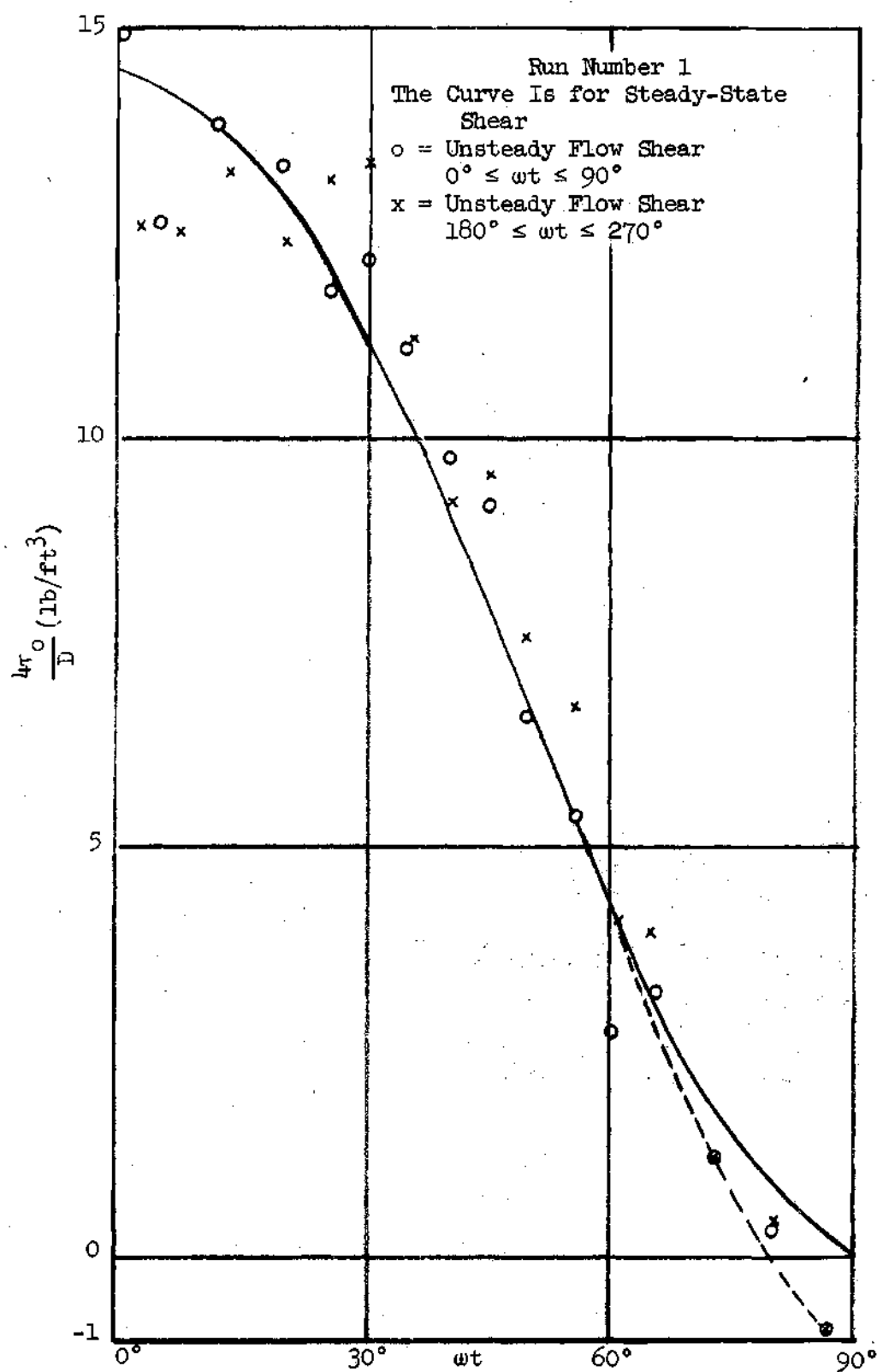
in which

$$R - \text{the Reynolds number} = \frac{VD}{\nu}$$

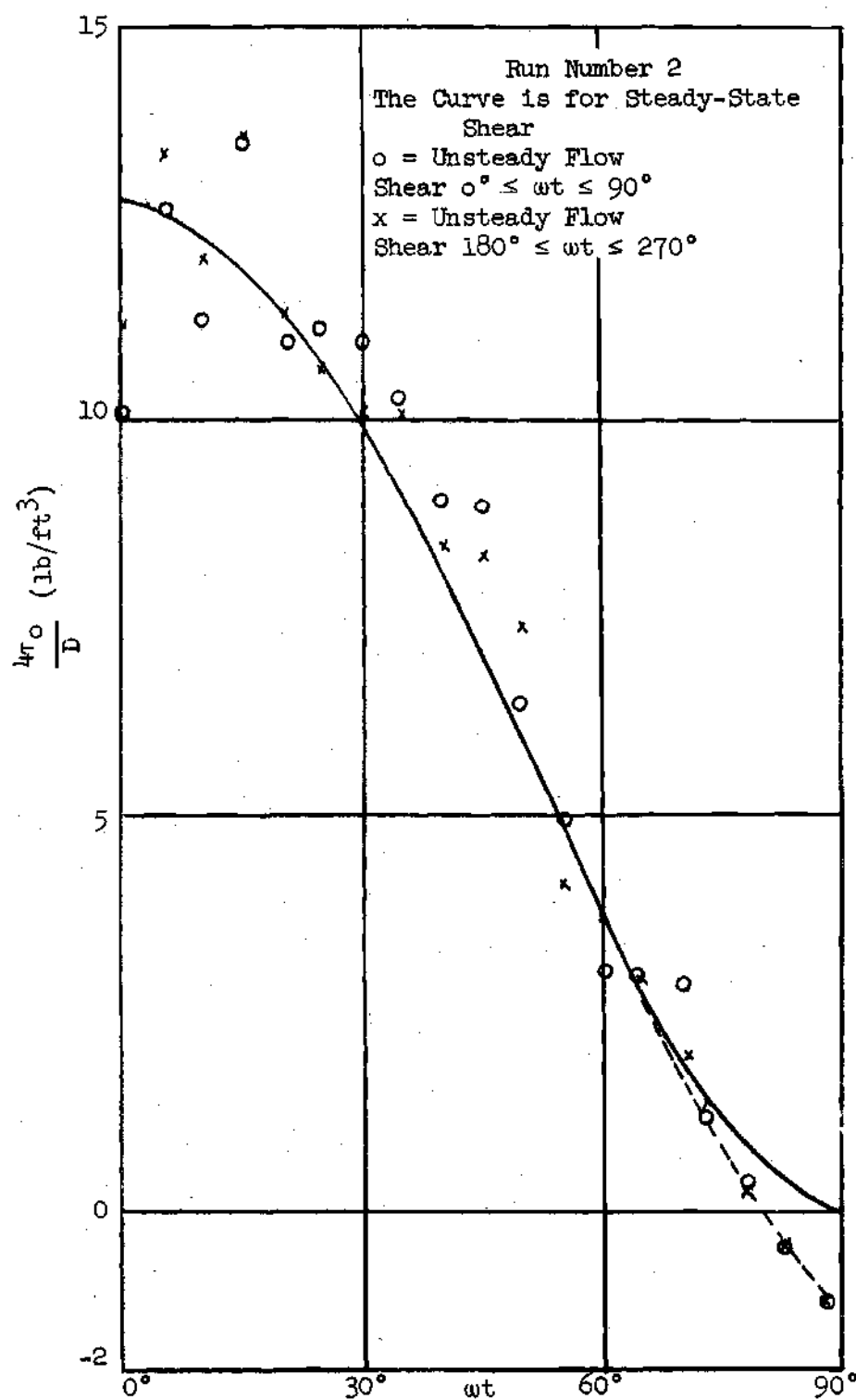
Putting this value of  $f$  into the Darcy-Weisbach equation and letting  $V = a_0 \omega \cos \omega t$ , then, for the experiments performed in this thesis, the equation takes the form,

$$\frac{4\tau_s}{D} = 15.16 (\cos \omega t)^{1.75}$$

This equation is solved for values of  $\omega t$  ranging from  $0^\circ$  to  $90^\circ$ . The numerical solution is shown in Figures 10, 11, and 12.

Figure 10. Plot of Shear Versus  $\omega t$  (Run No. 1)



Figure 11. Plot of Shear Versus  $\omega t$  (Run No. 2)

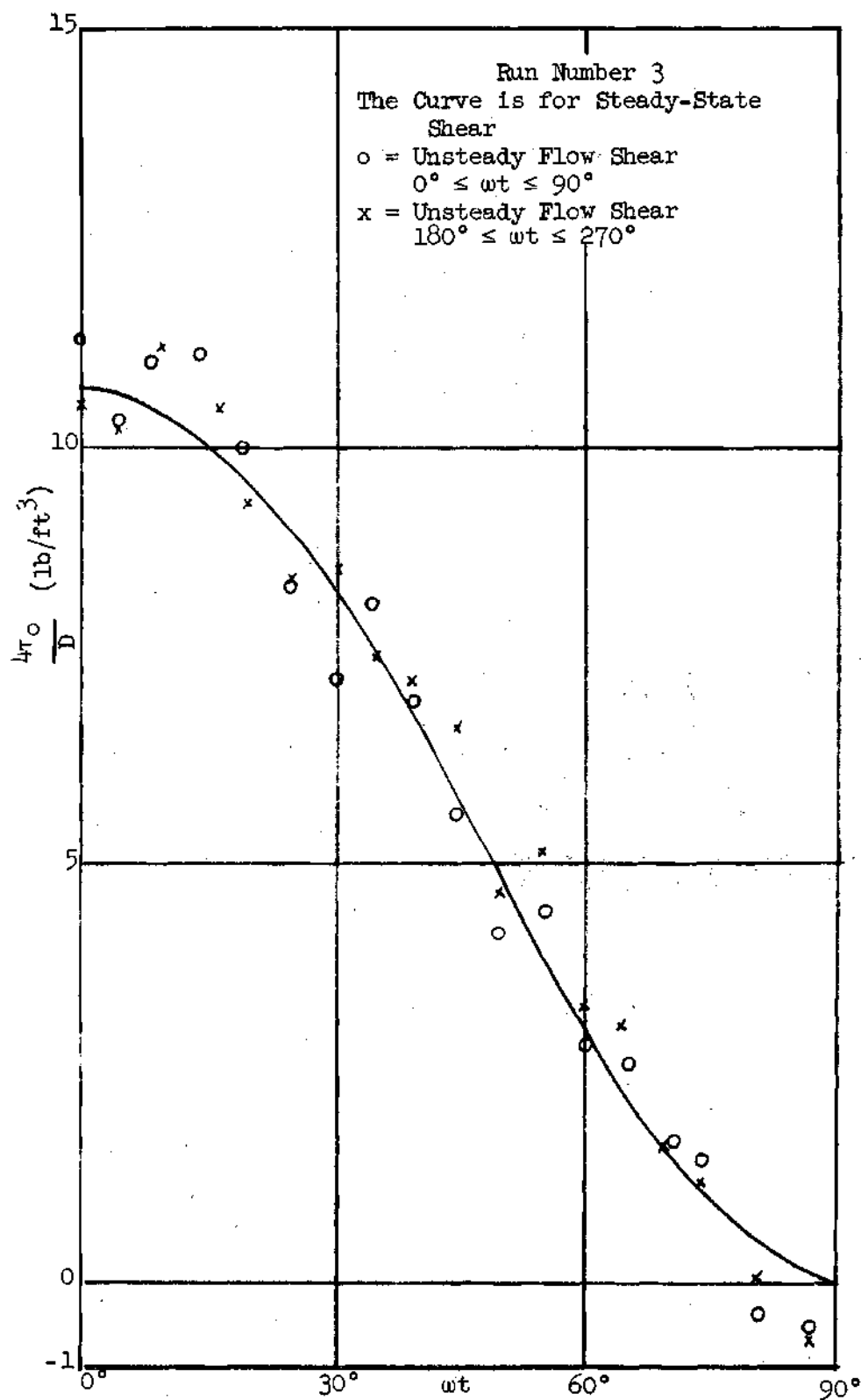


Figure 12. Plot of Shear Versus  $\omega t$  (Run No. 3)

## CHAPTER VI

### ANALYSIS OF DATA

The analysis of the data is broken into two distinct and separate steps which are a) a plotting of a pressure calibration curve for the transducers and b) an analysis of the pressure time record obtained for one complete cycle of the fluid in the test section. Each step will be discussed separately.

#### Pressure-Record Calibration

The pressure-record calibration consists of relating the pressure difference across the transducers to the distance from the bottom grid line on the record to the scribe line on the record,  $y$ . The values of pressure difference in cm of mercury and stylus deflection corresponding to this pressure difference for the runs analyzed in this thesis are presented in Table 1.

#### Discussion of Results

As shown in Figure 9, the value of  $4\tau_0/D$  is readily attainable for decelerated flows. However, when the fluid is accelerating, there is no method to accurately predict the value of  $4\tau_0/D$  using the equipment employed in these experiments. The reason was that intense fluctuations in the pressure record existed when the fluid was accelerating (Figure 8). The probable causes of these fluctuations will be discussed in a later paragraph.

Table 1. Calibration Data

Point	When Obtained	Oscillograph Chart Deflection in cm.	Differential Manometer Deflection in cm of Mercury
A	Before Experimental Run	2.25	0.000
B	" " "	2.80	-4.500
C	" " "	3.22	-7.875
D	" " "	3.50	-10.170
E	" " "	3.73	-12.025
F	" " "	4.50	-18.675
G	" " "	5.14	-25.695
H	" " "	0.83	12.115
I	" " "	0.38	16.845
J	" " "	1.43	6.735
K	" " "	1.65	4.880
L	After Experimental Run	2.24	0.000
M	" " "	1.38	8.720
N	" " "	0.62	13.935
O	" " "	2.40	-1.450
P	" " "	3.73	-12.130
Q	" " "	4.70	-20.835

As shown in Figures 10, 11, and 12, the values of  $4\tau_o/D$  for decelerated flows are essentially equal to those obtained for equivalent steady flow.

The boundary shear force changed direction approximately ten degrees before the mean velocity. In order to explain this, a force analysis was applied to the annular fluid element, one boundary of which is the pipe wall. Figure 13 is a free body diagram of this element.

Summing forces in the axial direction--

$$p_1^* \pi D \Delta y - p_2^* \pi D \Delta y + (\tau_0 + \Delta \tau) \pi DL - \tau_0 \pi DL = \frac{\partial}{\partial t} \int_V \rho v dV$$

in which

$\Delta \tau$  = incremental shear stress and

$\Delta y$  = incremental distance normal to the wall.

If  $\Delta y$  is very small then  $\partial/\partial t \int \rho v dV = 0$ , and  $\lim_{y \rightarrow 0} \Delta \tau / \Delta y = \partial \tau / \partial y$ .

Solving for  $\partial \tau / \partial y$ ,

$$\frac{\partial \tau}{\partial y} = \frac{-(p_1^* - p_2^*)}{L}$$

in which  $\partial \tau / \partial y$  = shear stress gradient normal to wall.

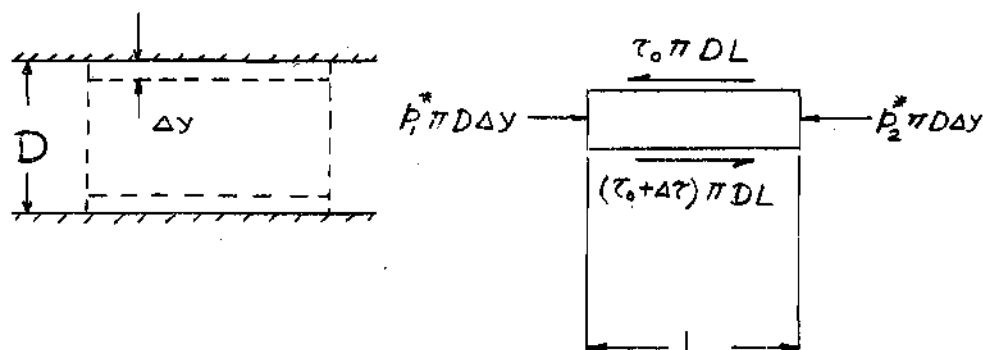


Figure 13. Free-Body Diagram of Annular Fluid Element Adjacent to Pipe Wall

Figure 14 is a plot of  $\partial v / \partial y$  versus  $\omega t$  for decelerated flows in the three experiments. Figure 15 is a qualitative interpretation of the shear distribution and velocity distribution at various critical values of  $\omega t$  for run 1. As shown in Figure 15 it is apparent that, as  $\omega t$  increases, the fluid near the boundary decelerates and, at  $\omega t = 79^\circ$ , the fluid near the boundary, and hence the boundary shear force, reverses direction. The reason that the fluid adjacent to the boundary and the shear stress do not change direction the same time as the pressure gradient ( $\omega t = 46^\circ$ ) is the fact that the adjacent fluid particles exert a shear stress opposite to the pressure gradient. This shear stress is sufficient to overcome the pressure gradient until  $\omega t = 79^\circ$  (the point where the shear force reverses).

#### Discussion of Fluctuations in the Pressure Record

The intense fluctuations in the pressure record when the fluid is accelerating may be attributable to three possible causes: a) mechanical vibrations, b) the natural frequency of the water columns in the piezometers or c) vortex generation in the fluid.

There are definitely vibrations of mechanical origin in the equipment due to vibrations in the motor. These vibrations are transmitted to the piezometers through the test section and the fluid itself. Referring to Figure 8, these vibrations appear as the periodic, small-scale oscillations throughout the pressure record. The methods tried to alleviate this problem were: a) the installation of a flexible link between the piezometers and the transducer, and b) sandbagging the test section. However, these measures were to no avail since the vibrations were transmitted through the fluid.

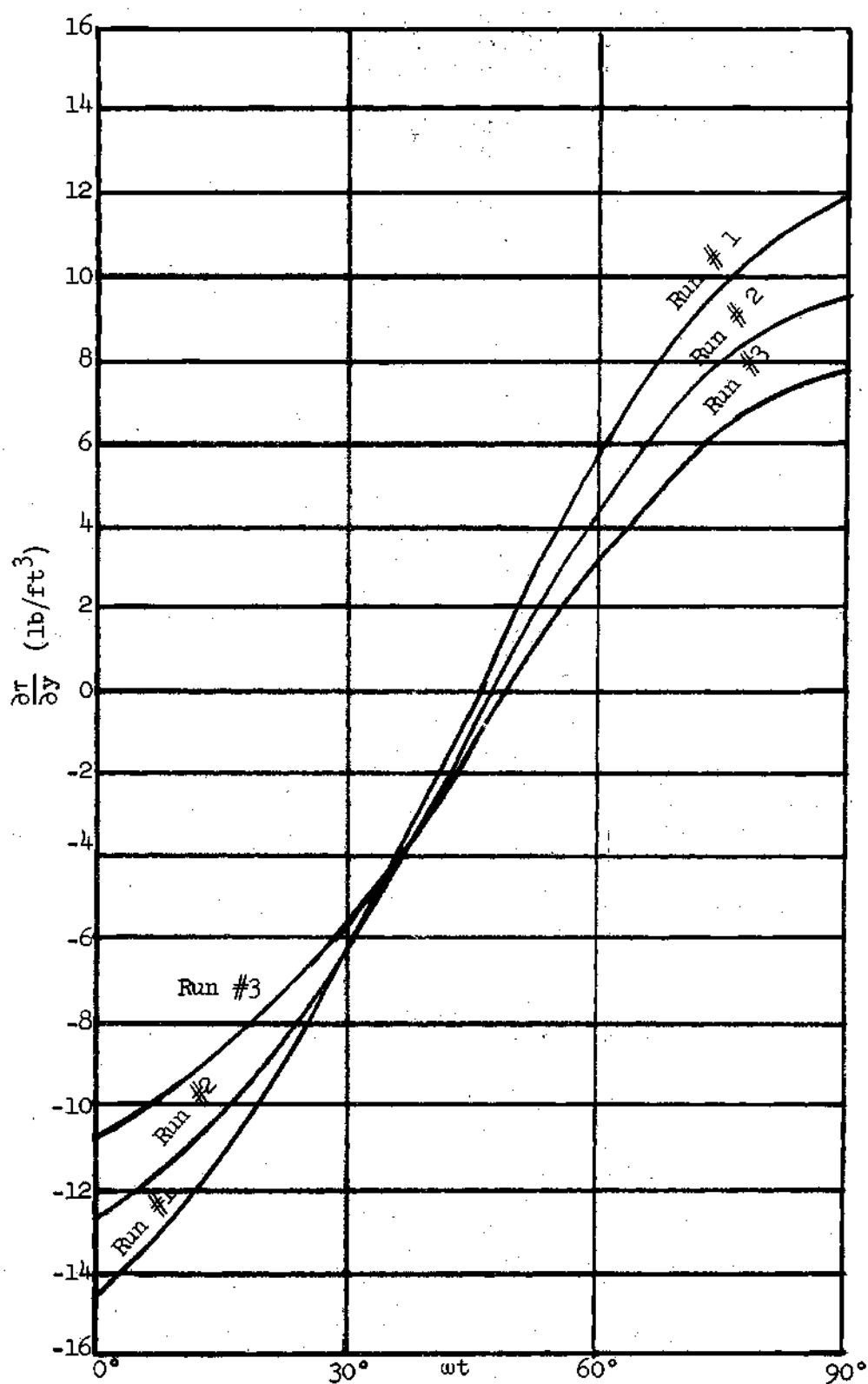


Figure 14. A Plot of Shear Stress Gradient Versus  $\omega t$  for Decelerated Flow

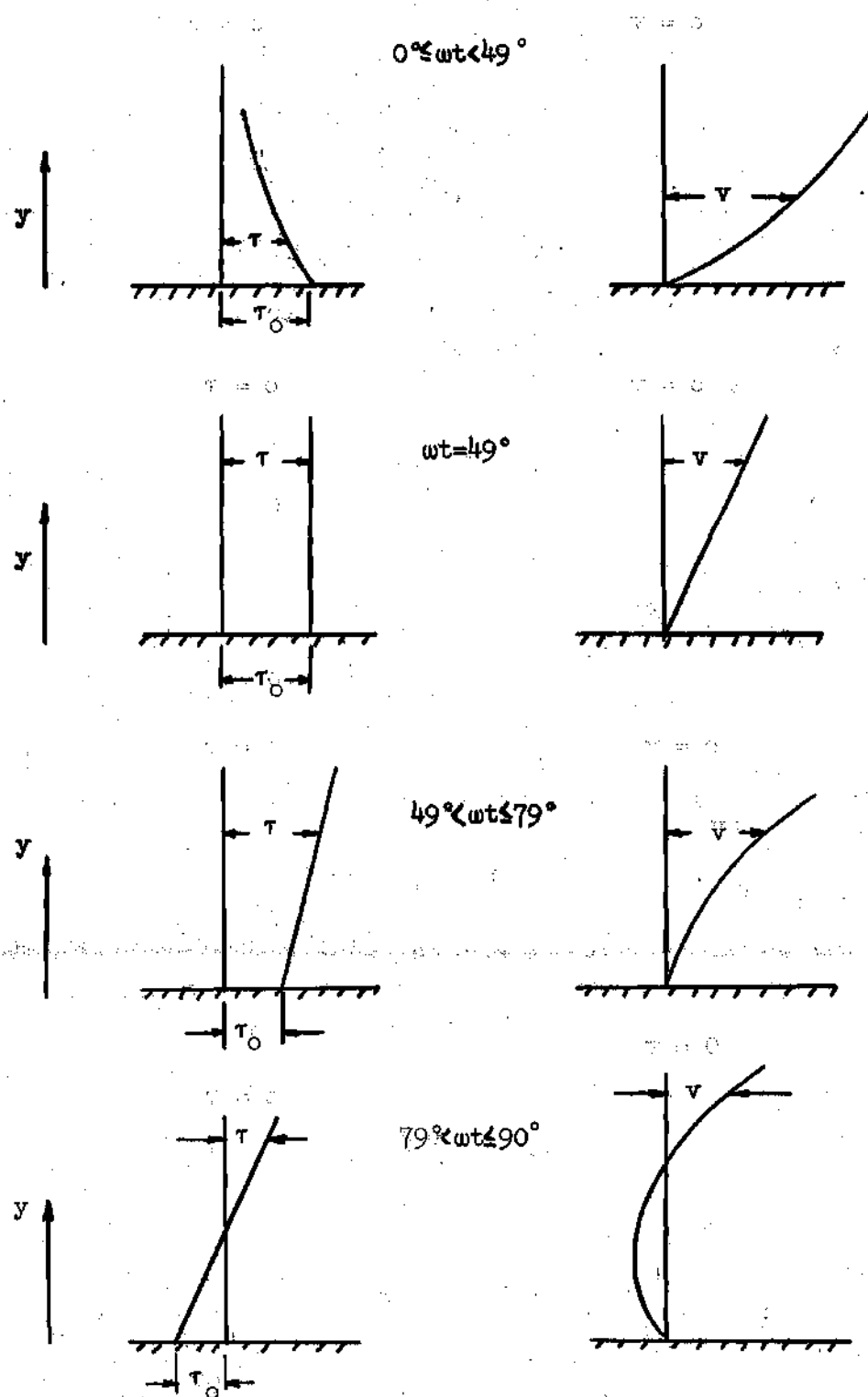


Figure 15. Shear and Velocity Profiles for Experiment 1



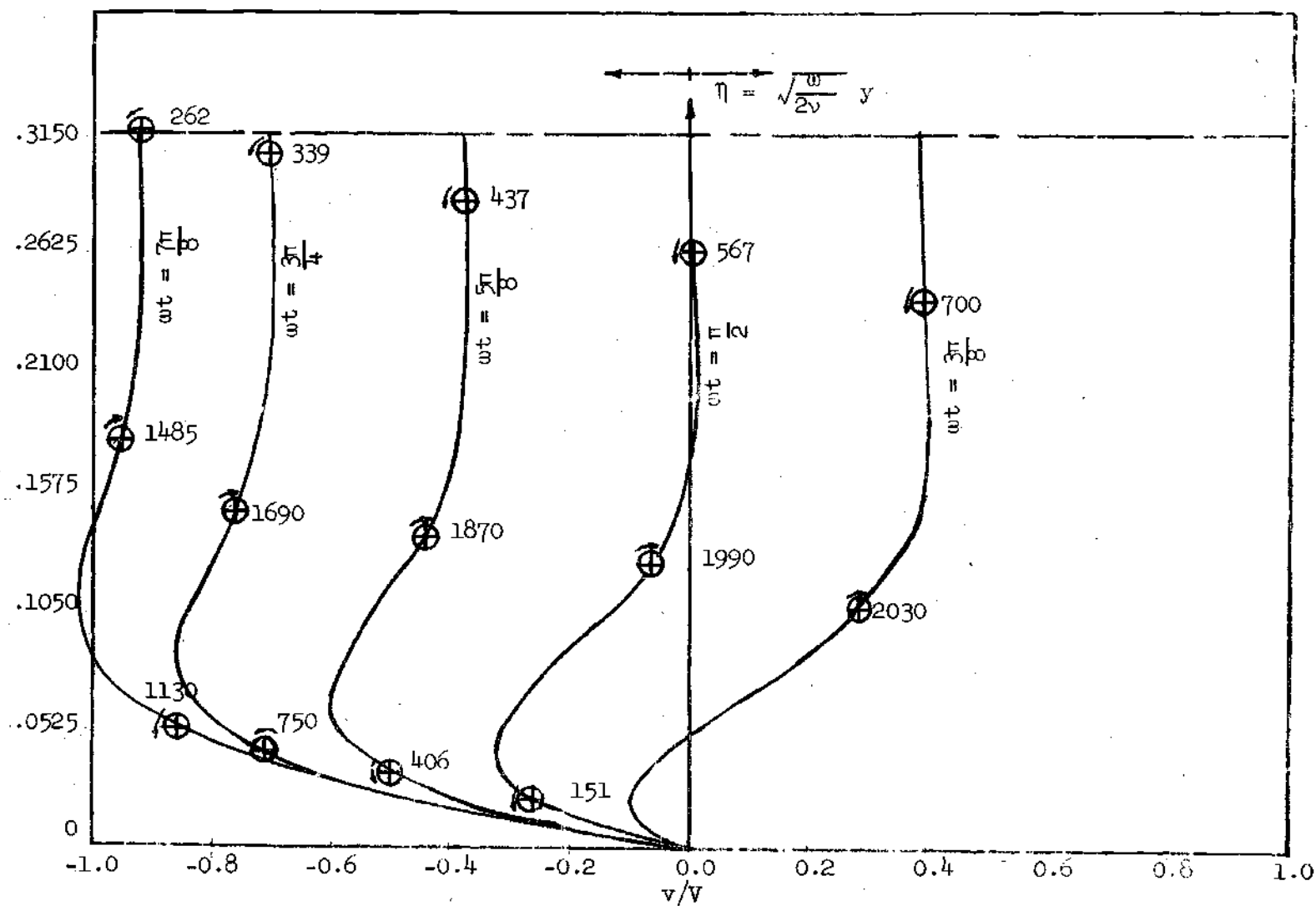


Figure 16. The Theoretical Velocity Profiles of Laminar Flow for Various Values of  $\omega t$

by the pressure transducer would be a function of the strength of the vortices. In any event, the time of occurrence of the pressure fluctuations ( $\omega t = 95^\circ$  in Figure 9) is in close agreement with the time of vortex formation ( $\omega t = \frac{5\pi}{8} = 112^\circ$  in Figure 16)

The measured pressure fluctuation occurring shortly after mean flow reversal could be the result of erratic movement of the piston or could be from the generation of vortices close to the boundary. Experimental evidence, which is currently available, is insufficient to distinguish between these two possible causes.

## CHAPTER VII

## CONCLUSIONS

The following conclusions are reached from the results of the experiments performed. For decelerated flows:

- (a) The steady-flow values for boundary shear stress are excellent approximations for decelerated flow.
- (b) The boundary shear stress in oscillatory turbulent flow changes direction approximately ten degrees before the mean velocity.

No values for the boundary shear stress can be obtained using this equipment when the fluid is accelerating. This is due to the intense fluctuations in the pressure record. More study should be devoted to the stability approach as a possible explanation for this phenomenon.

## BIBLIOGRAPHY

1. Carstens, M. R. and Roller, John E., "Boundary-Shear Stress in Unsteady Turbulent Pipe Flow," Journal of the Hydraulics Division, Proceedings of the American Society of Civil Engineers, Feb., 1951, pp. 67-81.
2. Dailey, J. W., Hankey, W. L., Jr., Olive, R. W., and Jordaan, J. M., Jr. "Resistance Coefficients for Accelerated and Decelerated Flows through Small Tubes and Orifices," Transactions, American Society of Mechanical Engineers, Volume 78, July 1956, pp. 1071-1077.
3. Sneddon, I. N., Fourier Transforms, McGraw-Hill Book Co., 1951, pp. 202-204.
4. Martin, C. S., Transition of Oscillatory Boundary-Layer Flow, Unpublished Paper, Georgia Institute of Technology, 1963.
5. Rouse, H., Elementary Mechanics of Fluids, John Wiley & Sons, Inc., New York, 1946, pp. 171-172.